THE STRUCTURES OF SOME EXTRAGALACTIC SOURCES AT 5000 MHz

By J. V. WALL* and D. J. COLE*

[Manuscript received 16 April 1973]

Abstract

The large scale structures of 30 extragalactic sources have been investigated using the Parkes 64 m telescope at 5000 MHz. Contour maps are presented for the resolved sources and comparisons are made with observations at lower frequencies.

I. INTRODUCTION

In this paper we present structural data for 30 sources obtained from 5000 MHz observations with a pencil beam of half-power width 4'·0 arc. Twenty-two of the sources were chosen from surveys of source structure carried out with the Parkes interferometer by Ekers (1969) and the present authors with D. K. Milne. Some of the present observations were undertaken to assist in the interpretation of this interferometry. A brief description of the observations and the method of analysis is given in Section II, the results are given in Section III, and a comparison with published data for lower frequencies is given in Section IV.

II. OBSERVATIONS AND ANALYSIS

The present observations were made with the Parkes 64 m telescope, which was equipped with the 5000 MHz receiver developed by J. W. Brooks and M. W. Sinclair of the Division of Radiophysics, CSIRO. The receiver was switched between two feeds, which produced two circular beams of 4'·0 arc half-width, one being on-axis and the other 18' arc off-axis. The system noise temperature of 80 K and bandwidth of 500 MHz yielded a peak to peak noise fluctuation of 0·07 f.u.† for an output time constant of 1 s.

The 22 sources selected from the Parkes interferometer surveys were observed in a two day session. Before the observation of each source a calibration signal of 1 K (2 f.u.) was injected at the receiver input and the resulting increase in receiver output was recorded by a PDP-9 on-line computer. Single scans in right ascension at $0^{\circ}\cdot 25\ \mathrm{min}^{-1}$ were made across the source at successive declinations spaced by between 1'·5 and 3'·0 arc, depending upon the extent of the source. During each scan the receiver output was sampled by the computer, and a digital filter was applied to the stored scan to attenuate spatial frequencies greater than those present in the telescope beam. The filtering resulted in a slight loss in resolution, effectively increasing the half-power beamwidth to 4'·1 arc. The computer then fitted a linear baseline to the end points of the scan to remove any gradient due to receiver drift.

* Division of Radiophysics, CSIRO, P.O. Box 76, Epping, N.S.W. 2121.

† 1 flux unit (f.u.) = $10^{-26}\ \mathrm{W\,m^{-2}\,Hz^{-1}}$.

Scans thus processed were plotted at successively greater base levels on an X–Y recorder in order to provide an on-line representation of the source structure. Contour maps for the well-resolved sources were subsequently drawn from these plots. In order to obtain the same intensity scale for the maps as that adopted by Shimmins *et al.* (1969), peak flux densities were first computed from the plots using a nominal value of 2 f.u. for the calibration signal. Small corrections were then applied to remove the zenith angle dependent effects of atmospheric attenuation and aperture efficiency. The resulting flux densities for 10 sources were compared with the corresponding results obtained by Shimmins *et al.* in order to determine the flux density scaling factor. The r.m.s. scatter about the mean ratio was found to be 3%. A calibration of the telescope pointing was carried out prior to the observations and the requisite corrections to the dial coordinates were incorporated in the final contour maps.

The eight additional sources were mapped during observing sessions in which positions and flux densities of large numbers of sources in the Parkes catalogues were obtained (Shimmins and Bolton 1972; unpublished Parkes data). The observations were made by taking forward–reverse scan pairs through each source at a scan spacing of $2'\cdot 0$ arc. These scans were made in the coordinate of maximum source extension, with a few "tie-down" scans being made in the other coordinate. A scan rate of $0^{\circ}\cdot 25\ \mathrm{min}^{-1}$ and an output time constant of 1 s were used. The scans were recorded on strip chart along with the deflections produced by the calibration signal, which was injected at the receiver input several times during the observation of each source. The contour maps were constructed from these analogue records. In the intensity scaling, appropriate corrections were again applied for zenith angle dependent factors, and the value of the calibration signal in flux units was determined by observations of flux density calibrator sources during the course of the observing session. Likewise the pointing calibration carried out in the session was used to apply the requisite corrections to dial coordinates in the drawing of the final maps.

III. Source List

The results of the observations together with relevant data on the sources are given in Table 1. Source designations are given in columns 1 and 2. For 24 of the 30 sources, the position coordinates (columns 3 and 4) which were measured with the Parkes 64 m telescope at 2650 MHz (Shimmins *et al.* 1966; Shimmins 1968) refer to the emission centroid. The remaining six "sources", PKS 0148−29, 0149−29, 1107−22, 1354−17, 1518−29, and 2329−16 appear to be composed of two or more unassociated sources, the positions of which were determined from the present observations. The r.m.s. error in each coordinate for these positions and for the emission centroids of the contour maps is 20″ arc unless otherwise noted in the table.

Optical identifications for the sources are given in column 5. Most of these are taken from Parkes identification papers but references to other papers, where applicable, are given in Section IV. Abbreviations used in column 5 and Section IV are: Sp, E, N, D, db, galaxies of the corresponding optical type; QSO, quasi-stellar object; and QSO?, possible quasi-stellar object.

The r.m.s. error in the peak flux density given in column 6 is the sum of 3% of this flux density and a constant $0\cdot 02$ f.u. The integrated flux density values given in column 7 were obtained by planimetry of the contour maps for the well-resolved sources or by calculation from the observed beam broadening for the poorly resolved sources. The three values enclosed by square brackets were obtained by application of the size factors computed by Shimmins *et al.* (1969) to the measured peak flux densities.

Column 8 contains the figure number of the contour map which is presented for the resolved sources. The contour interval (in flux units and brightness temperature) is indicated in the figure captions. A dashed outer contour indicates an intensity level of half the contour interval. The r.m.s. error at each point on the maps due to receiver fluctuations, gain instabilities, and smoothing and baseline fitting procedures is the sum of 2% of the peak intensity and 0·02 K (or 0·02 f.u.). The contours are intensity isophotes for one linear polarization only, the position angle of observation being chosen so that the off-axis beam did not encounter the source during the scans. However, the contours are believed to represent total intensity to within a few per cent, since the high degrees of linear polarization found by Gardner and Whiteoak (1971) at 5000 MHz are in regions of low surface brightness in very extended sources.

Column 9 contains a summary of the structure of each source as obtained in the present work and from published observations (for which references are given). Abbreviations used in column 9 and in the more detailed comparison of results given in Section IV are: N, north; S, south; E, east; W, west; PA, position angle; comps, components; diams, diameters; and coords, errors in position coordinates. (Abbreviations of the references are given at the end of the table.)

IV. Source Structures

PKS 0045 − 25

The source PKS 0045 − 25 was identified with NGC 253, the brightest southern spiral, by Mills (1955). From observations with interferometers, both Ekers (1969) and Fomalont (1971) proposed models of the core–halo type, with the compact core of dimensions ~1′ arc and the extended halo of dimensions in the range 4′ to 7′ arc. Because of the discontinuity between the fringe visibility functions obtained at 467 and 1401 MHz, Ekers suggested that the halo has a steeper emission spectrum than the core.

The source is poorly resolved in the present observations (Fig. 1(*a*)) but the contours indicate extension along PA 50°. A clear indication of the change in structure with frequency suggested by Ekers (1969) is provided in a comparison of these observations with the structure determined by Cameron (1971) at 408 MHz and by Slee (1972) at 80 MHz. Using the Molonglo Cross of the University of Sydney (beamwidth 2′·6 arc) Cameron found that the source consists of three components centred on the nucleus of the galaxy: a compact core 0′·8 arc in width and two components, extended along the optical disc, of full EW widths 5′·7 and 16′ arc. With the radioheliograph of the Division of Radiophysics, CSIRO, (beamwidth 3′·7 arc) Slee found that these disc components account for 64% of the total emission from the galaxy at 80 MHz. At 408 MHz the disc components contribute 73% of the total emission. The 5000 MHz observations are consistent with a model in which the extended components found by Cameron and Slee contribute only ~20% of the total emission. Figure 1(*b*) shows the spectra of the disc and nuclear components given by

TABLE 1

SOURCE LIST

(1) Parkes catalogue number	(2) Other designation	(3) Position (1950) R.A. h m s	(4) Dec. ° ′ ″	(5) Identification	(6) S_{5000} Peak (f.u.)	(7) Integ. (f.u.)	(8) Map (Fig.)	(9) Description* of structure
0045 − 25	MSH *22*, NGC 253	00 45 04·9	−25 33 33	Sp $7^m\cdot0$ (NGC 253)	2·03	2·40	1	Three comps centred on nucleus, one compact (0′·8 to half-power), the others extended along disc; structure is frequency dependent (C, S, F2, E)
0055 − 01	MSH *17*, 3C 29, 4C − 1·05, NRAO 50	00 55 01·0	−01 39 35	E $15^m\cdot6$	2·17	[2·56]		1′·1 × 2′·5 (EW × NS) (F1, M)
0105 − 16	MSH *2*, 3C 32, NRAO 55	01 05 48·0	−16 20 21		1·04	[1·09]		Double structure EW, comps < 0′·6, sepn. 0′·75, < 0′·8 NS (F1, M)
0123 − 01	MSH *5*, 3C 40, 4C − 1·08, NRAO 70, NGC 545-547	01 23 27·8	−01 38 29	db $13^m\cdot2$ (NGC 545-547)	0·92	2·25	2	Two main comps, sepn. ~ 6′ along PA 178°, together with complex low-level emmission regions; structure is frequency dependent (F1, M, S3, L)
0148 − 29	MSH *17*? {0148 − 29·8	01 48 28·0	−29 48 09			0·97		Double structure EW, sepn. 0′·9 (F1)
	0148 − 29·5	01 48 32·0	−29 35 45			0·15		< 2′ × < 3′ (EW × NS), coords ± 30″
0149 − 29	MSH *17*? {0149 − 29	01 49 45·0	−29 55 53			0·36		< 1′ × < 2′ (EW × NS), coords ± 30″
	0150 − 29	01 50 17·5	−29 57 35			0·30		< 1′ × < 2′ (EW × NS), coords ± 30″
0331 − 01	MSH *3*, 3C 89, 4C − 1·12, NRAO 139	03 31 41·8	−01 21 10	D $18^m\cdot3$	0·67	0·76		Two comps, diams < 0′·6, intensity ratio 2·5, sepn. 2′·0 along PA ~ 70° (F1)
0349 − 14	MSH *9*, 3C 95, NRAO 147	03 49 09·7	−14 38 18	QSO $16^m\cdot2$	0·68	0·74	3	Two comps, diams < 0′·8, sepn. 1′·8 along PA 166°, intensity ratio 1·8 (F2, M)
0349 − 27	MSH *12*	03 49 32·6	−27 53 05	E $16^m\cdot8$	1·36	2·01	4	Three comps along PA 56°, total sepn. 4′·6; structure is frequency dependent (F2, E, L)
0431 − 13·5	MSH *12*?, NRAO 185	04 31 49·3	−13 28 58	E $16^m\cdot3$		0·28		< 0′·4 (F1) × < 2′ (EW × NS)
0431 − 13·3	MSH *12*?	04 31 55·3	−13 16 58	E $18^m\cdot8$	0·40	[0·44]		Two comps, diams < 0′·5, sepn. 1′·4 along PA 38°, intensity ratio 1·2 (E); or single source 1′·6 × 2′·5 (EW × NS) (F1, M)
0454 − 22	MSH *21*	04 54 01·6	−22 04 06		0·89	0·92		~ 1′·5 × < 1′·0 (EW × NS)
0511 − 30	MSH *5*	05 11 38·2	−30 32 55	E $17^m\cdot0$	0·47	1·03	5	Three extended comps, total sepn. 7′·0 along PA 27° (F2, E, F1, L, S2)
0541 − 24	MSH *7*	05 41 09·9	−24 22 32	N $18^m\cdot0$		0·34		< 1′·3 × < 0′·9 (EW × NS)
0634 − 20	MSH *10*	06 34 22·0	−20 29 18	N $16^m\cdot8$	1·11	3·55	6	Two comps, sepn. 11′ along PA 178°, joined by an emission bridge (E, S2, G)
		06 34 23·1	−20 39 18		1·32			

(1) Parkes catalogue number	(2) Other designation	(3) Position (1950) R.A. h m s	(4) Dec. ° ′ ″	(5) Identification	(6) S_{5000} Peak (f.u.)	(7) Integ. (f.u.)	(8) Map (Fig.)	(9) Description* of structure
0800−09	MSH *13*	08 00 15·0	−09 49 50	E $18^m\cdot5$	0·36	0·96	7	Two comps, sepn. ~7′ along PA 90°; structure is frequency dependent (E, L, S2)
0806−10	MSH *4*, 3C 195, NRAO 283	08 06 30·6	−10 19 03	E $18^m\cdot8$	1·31	1·60	8	Two comps, dimensions 0′·5 × 0′·5, sepn. 1′·3 along PA 14°, intensity ratio 1·4 (F2)
0819−30	MSH *3*	08 19 25·8	−30 01 13	E3 $18^m\cdot2$	0·62	1·17	9	Three comps, total sepn. ~4′·5 along PA 126° (F2); or two comps, intensity ratio ~2·5, joined by an emission bridge (E, L, S1)
1107−22	MSH *3* {1106−22	11 06 42·9	−22 45 52			0·27		< 2′ × < 3′ (EW × NS)
	{1107−22	11 07 23·9	−22 46 22			0·11		< 3′ × < 4′ (EW × NS), coords ± 30″
1354−17	MSH *15* {1354−17·6	13 54 10·6	−17 37 22	QSO? $18^m\cdot5$		0·32		< 2′ × < 3′ (EW × NS), coords ± 30″
	{1354−17·4	13 54 21·0	−17 29 40			1·17		< 1′·2 × < 1′·5 (EW × NS)
1514−16		15 14 36·9	−16 30 47		0·32	0·54	10	Two comps, sepn. 6′·3 along PA 73°, peak intensity ratio 1·9
1518−29	{1518−29·5	15 18 44·4	−29 31 19			0·35		< 2′ × < 3′ (EW × NS), coords ± 30″
	{1518−29·6	15 18 56·2	−29 36 50			0·18		< 2′ × < 3′ (EW × NS), coords ± 30″
	{1519−29·4	15 19 19·5	−29 24 38			0·49		< 1′·5 × < 2′ (EW × NS)
	{1519−29·6	15 19 35·4	−29 38 45	E $18^m\cdot5$		0·22		< 2′ × < 3′ (EW × NS), coords ± 30″
1559+02	MSH *1*, 3C 327, 4C 02·41, NRAO 489	15 59 56·7	+02 06 20	D $17^m\cdot0$	2·16	2·81	11	Two comps, sepn. 3′·5 along PA 100° and extended along this line, intensity ratio 2·3 (F2, L)
1949−01	3C 403·1, 4C −1·51, NRAO 617	19 49 52·8	−01 25 15	E $17^m\cdot5$	0·28	0·62	12	Two comps, sepn. 3′·6 along PA 134°, peak intensity ratio 1·1
2058−28	MSH *15*	20 58 39·1	−28 13 49	E $15^m\cdot6$	1·26	1·96	13	Two comps, sepn. 3′·0 along PA ~160° and extended along this line, intensity ratio ~1·3 (F2, E, L)
2058−13	MSH *19*	20 58 56·7	−13 30 38	E3 $15^m\cdot2$	0·23	0·43	14	Two comps, sepn. 5′·5 along PA 101° and joined by an emission bridge, peak intensity ratio 1·5
2104−25	MSH *1*	21 04 24·9	−25 39 06	E $16^m\cdot8$	2·21	4·23	15	Two comps, similar intensities, sepn. ~4′ along PA ~20°; southern component is extended in PA ~135° with dimensions 6′ × 2′ (F2, E, L)
2149−20	MSH *21*	21 49 04·1	−20 00 26			0·70		< 0′·6 × < 0′·6 (EW × NS)
2221−02	MSH *9*, 3C 445, 4C −2·83, NRAO 685	22 21 15·6	−02 21 54	N $17^m\cdot5$	0·86	2·25	16	Two comps, sepn. ~4′ along PA ~170° and joined by an emission bridge (F1, M)
2329−16	{2328−16	23 28 41·2	−16 16 47			0·13		< 4′ × < 4′ (EW × NS)
	{2329−16	23 29 03·6	−16 13 29	N $18^m\cdot5$		1·02		< 0′·6 × < 1′·0 (EW × NS)

* Abbreviations of references are: C, Cameron (1971); E, Ekers (1969); F1, Fomalont (1968); F2, Fomalont (1971); G, Gardner and Whiteoak (1971); L, Lockhart (1971); M, Maltby and Moffet (1962); S1, Schilizzi and McAdam (1969); S2, Schilizzi and McAdam (1970); S3, Schilizzi *et al.* (1972); S, Slee (1972).

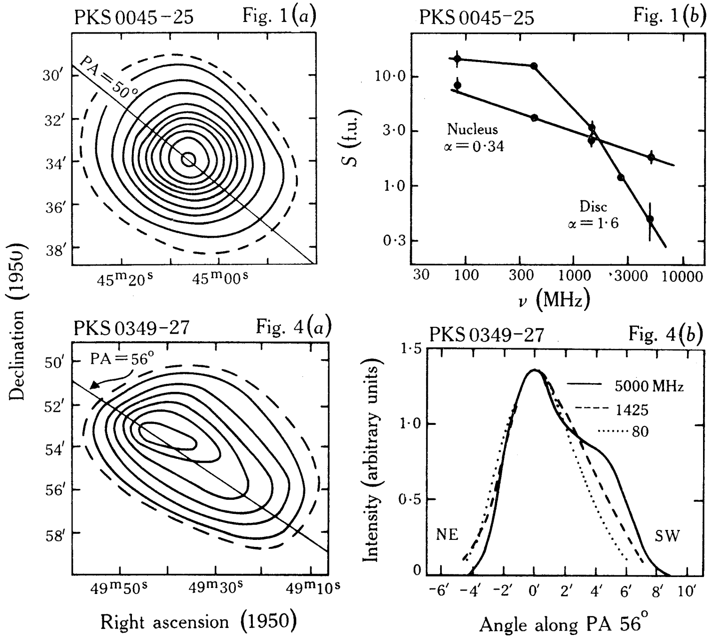

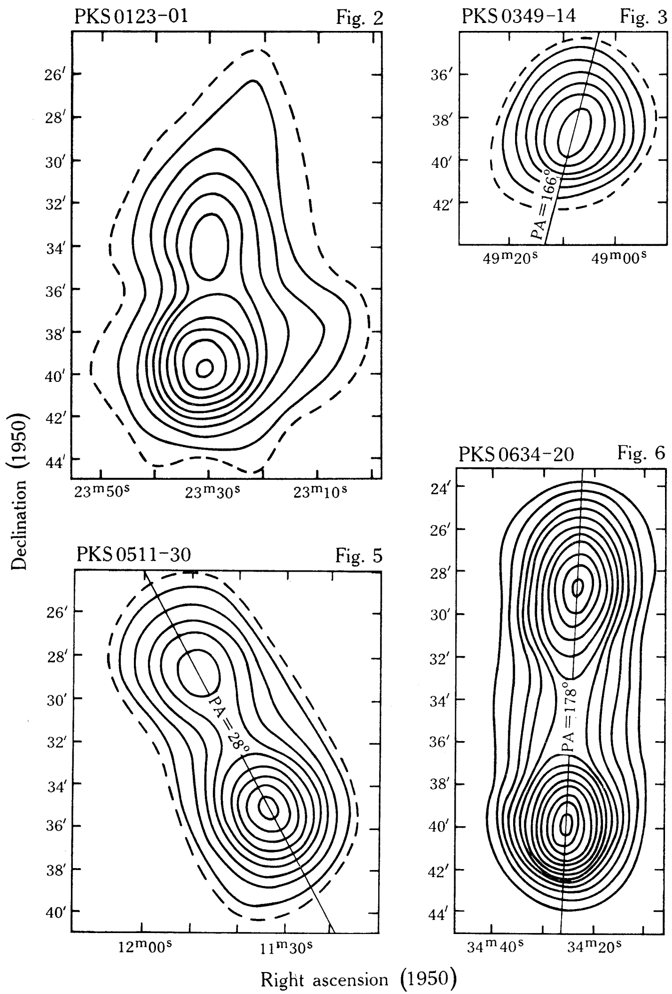

Fig. 1.—(*a*) 5000 MHz map of PKS 0045 − 25 in steps of 0·20 f.u. (0·17 K).
(*b*) Spectra of disc and nuclear components of PKS 0045 − 25 (NGC 253).

Fig. 2.—5000 MHz map of PKS 0123 − 01 in steps of 0·10 f.u. (0·08 K).

Fig. 3.—5000 MHz map of PKS 0349 − 14 in steps of 0·10 f.u. (0·08 K).

Fig. 4.—(*a*) 5000 MHz map of PKS 0349 − 27 in steps of 0·20 f.u. (0·16 K).
(*b*) Intensity distributions along PA 56° for PKS 0349 − 27.

Fig. 5.—5000 MHz map of PKS 0511 − 30 in steps of 0·05 f.u. (0·04 K).

Fig. 6.—5000 MHz map of PKS 0634 − 20 in steps of 0·10 f.u. (0·08 K).

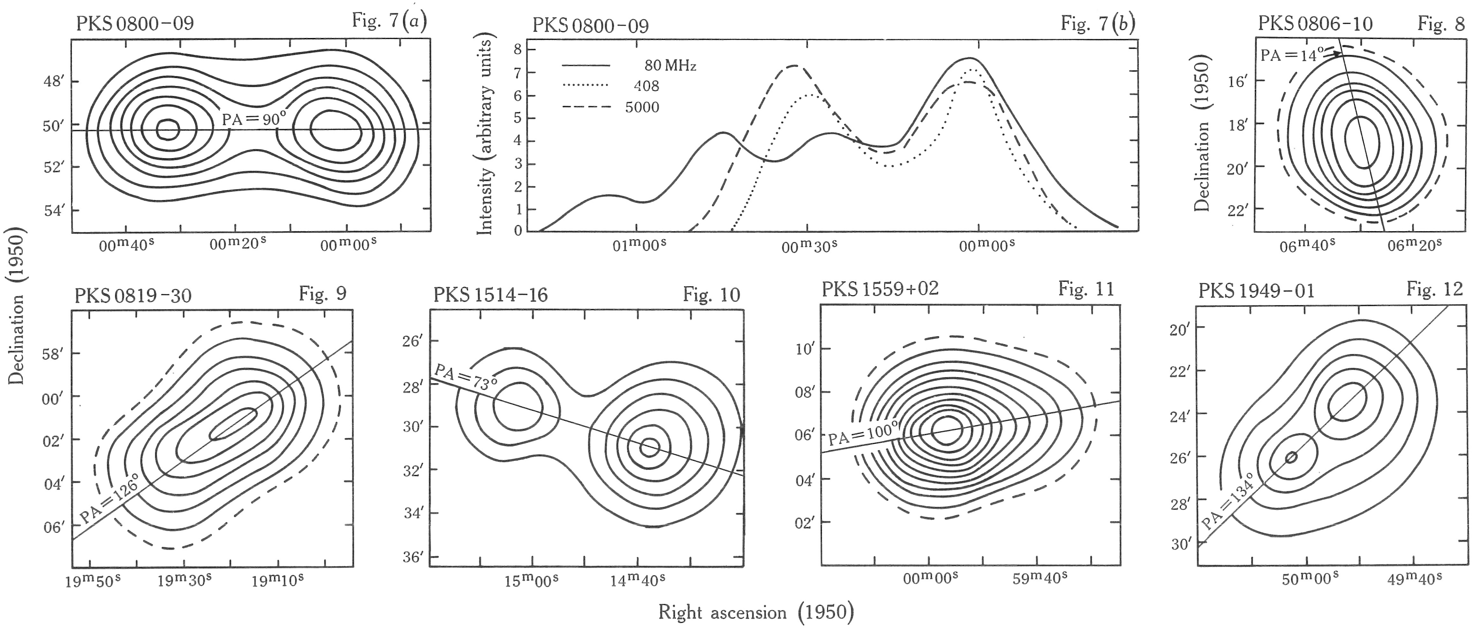

Fig. 7.—(*a*) 5000 MHz map of PKS 0800 − 09 in steps of 0·05 f.u. (0·04 K).
(*b*) Intensity distributions along PA 90° for PKS 0800 − 09.

Fig. 8.—5000 MHz map of PKS 0806 − 10 in steps of 0·20 f.u. (0·17 K).

Fig. 9.—5000 MHz map of PKS 0819 − 30 in steps of 0·10 f.u. (0·08 K).

Fig. 10.—5000 MHz map of PKS 1514 − 16 in steps of 0·05 f.u. (0·04 K).

Fig. 11.—5000 MHz map of PKS 1559 + 02 in steps of 0·20 f.u. (0·17 K).

Fig. 12.—5000 MHz map of PKS 1949 − 01 in steps of 0·05 f.u. (0·04 K).

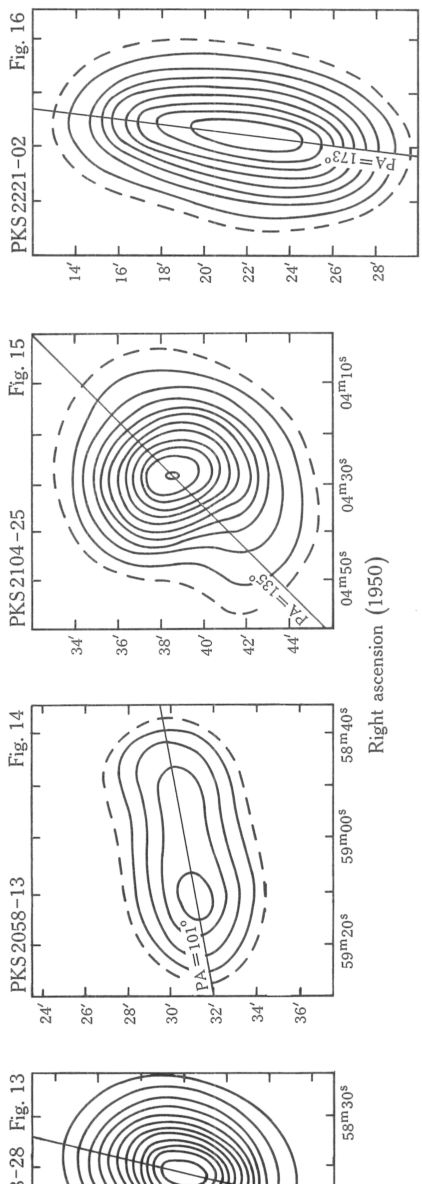

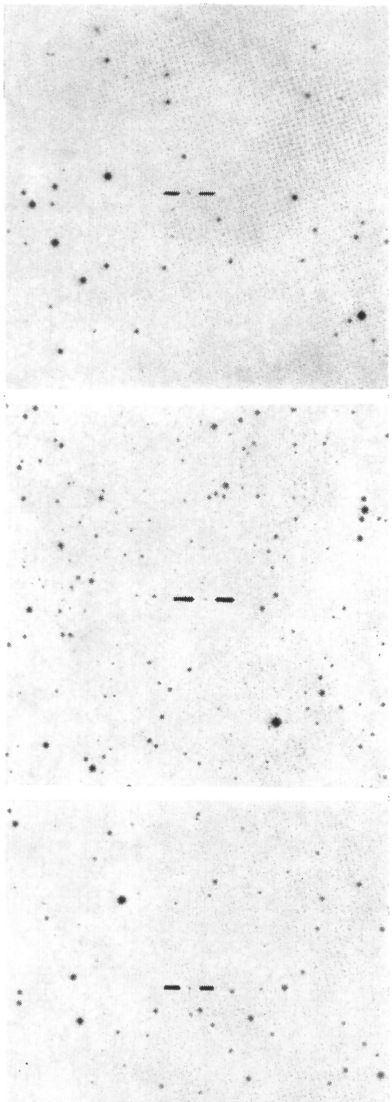

Fig. 17 (a) PKS 1354−17·6

Fig. 17 (b) PKS 1519−29·6

Fig. 17 (c) PKS 2329−16

Slee (1972; his Figure 3) with the addition of points at 5000 MHz determined from the present work. The extended components lying along the major axis of the optical disc account for the unsatisfactory interpretation of the interferometry provided by a core–halo model with Gaussian brightness distributions (Fomalont 1971).

PKS 0055 − 01

The present observations of PKS 0055 − 01 show some beam broadening indicative of source dimensions $\sim 0'\cdot 8 \times \sim 1'\cdot 6$ (EW × NS). These results are in reasonable agreement with previous investigations of the structure. From observations with the Caltech interferometer, Maltby and Moffet (1962) concluded that the source is $2'\cdot 5$ arc NS "with the possibility of some structure", while Fomalont (1968) suggested that the source consisted of a single component $1'\cdot 1$ arc EW.

PKS 0105 − 16

From the present observations of PKS 0105 − 16, upper limits to the angular dimensions of the source are $0'\cdot 8 \times 0'\cdot 5$ (EW × NS). These limits are consistent with results from the Caltech interferometer, which indicate an overall dimension of $0'\cdot 8$ arc NS (Maltby and Moffet 1962) and two small-diameter components in the EW direction separated by $0'\cdot 75$ arc (Fomalont 1968).

PKS 0123 − 01

Mills (1960) identified the source PKS 0123 − 01 with the double galaxy NGC 545–547, a close pair of 13^m ellipticals. In a recent study of the structure of PKS 0123 − 01, Schilizzi *et al.* (1972) compared the present 5000 MHz map (Fig. 2) with 408 and 80 MHz maps obtained from observations with similar resolution and found a marked dependence of structure on frequency. The two main components, separated by $\sim 6'$ arc NS, have a spectral index* of $\sim 0\cdot 6$, while to the north and south of these components there are low-level emission regions of spectral index $\sim 1\cdot 0$. These outer regions may represent a pair of older components in which the spectrum has been steepened with the modification of the synchrotron emission by processes of diffusion and/or adiabatic expansion. The age of each pair of components was estimated by Schilizzi *et al.* as between 10^6 and 10^7 yr and the average rate of supply of energy to them to be $\sim 5 \times 10^{51}$ erg yr^{-1}. These values are similar to those found for emitting regions of other radio galaxies. The contour maps also indicated that there is radio emission from NGC 541, a third 13^m elliptical galaxy $4'\cdot 6$ arc south-west of NGC 545–547. Schilizzi *et al.* suggested that this emission was generated by relativistic particles from NGC 545–547.

* The spectral index α is defined from $S_\nu \propto \nu^{-\alpha}$, where S_ν is the flux density at the frequency ν.

Fig. 13.—5000 MHz map of PKS 2058 − 28 in steps of 0·10 f.u. (0·08 K).
Fig. 14.—5000 MHz map of PKS 2058 − 13 in steps of 0·05 f.u. (0·04 K).
Fig. 15.—5000 MHz map of PKS 2104 − 25 in steps of 0·20 f.u. (0·17 K).
Fig. 16.—5000 MHz map of PKS 2221 − 02 in steps of 0·10 f.u. (0·08 K).
Fig. 17.—Finding charts for the new optical identifications prepared from the Palomar Sky Survey prints. The scale is 5 mm ≈ 1′ arc, and north–east is at the upper left hand corner. Part (*a*) for PKS 1354 − 17·6 (QSO?) is from the blue print and parts (*b*) for PKS 1519 − 29·6 and (*c*) for PKS 2329 − 16 (galaxies) are from the red prints.

PKS 0148 − 29 and 0149 − 29

Scans to map the region about PKS 0148 − 29 and 0149 − 29 revealed the four apparently unassociated sources listed in Table 1. The strongest of these may have EW structure 1′ to 2′ arc in extent. Observations with the Caltech interferometer (Fomalont 1968) indicated that PKS 0148 − 29 has two components with EW separation 0′·9 arc, which is in agreement with the present results. However, the conclusion that the EW extent of PKS 0149 − 29 is less than 1′·0 arc (Fomalont 1968) is incorrect as the "source" PKS 0149 − 29 is actually two sources separated by 7′·2 arc along PA 103°. The Palomar Sky Survey prints were examined at each of the four source positions but no optical identifications could be made.

PKS 0331 − 01

From observations of PKS 0331 − 01 with the Caltech interferometer Fomalon (1968) derived a model for the EW structure consisting of two small-diameter components with intensity ratio 2·5 and separated by 0′·8 arc. The EW beamwidth (4′·3 ± 0′·1 arc) observed in the present measurements is in good agreement with this interpretation. Along PA 80° ± 10° the beam broadening in the present observations is maximum, the width being 4′·5 ± 0′·2 arc. A model consistent with this result and with the interferometry consists of two components of widths <0′·6 arc and intensity ratio 2·5 separated by 2′·0 arc along PA 70°. The stronger component is to the south–east.

PKS 0349 − 14

There is excellent agreement between the intensity profile of PKS 0349 − 14 along PA 166° from the brightness distribution of Figure 3, and a profile along this position angle obtained by convolving the model proposed by Fomalont (1971) (Table 1) to the present resolution. The source is identified as a 16^m QSO (Bolton and Ekers 1966*a*) with a redshift of 0·614. If this redshift is cosmological in origin, the 1′·8 arc angular separation of the components indicates a physical separation of between 275 and 590 kpc for the range of cosmological models considered by McVittie (1965). Consequently, the separation of the components may exceed that for PKS 1233 − 24 (Wall *et al.* 1968), the largest previously reported for a QSO.

PKS 0349 − 27

Fomalont (1971) interpreted his observations of PKS 0349 − 27 with the Caltech interferometer in terms of a model with three Gaussian components (Table 1). However, his Figure 3(*d*) suggests that "components" B and C may represent a single extended region of emission. There is general agreement between this model and the results obtained by Ekers (1969) with the Parkes interferometer. The brightness distribution obtained from the present observations is shown in Figure 4(*a*) and a profile of the brightness distribution along PA 56° is shown in Figure 4(*b*). Two other such profiles along this position angle are also shown: that obtained by Lockhart (1971) at 80 MHz with resolution similar to that of the present observations, and that obtained by convolving Fomalont's (1971) model of the emission at 1425 MHz to the resolution of the present observations. There is a clear indication of change in structure with frequency. The south–west component has a markedly flatter emission spectrum ($\alpha \approx 0 \cdot 6$) than the north–east component ($\alpha \approx 0 \cdot 8$). Searle and Bolton (1968) noted that two jets showing emission lines extend from the elliptical galaxy identified with the source, and that the more prominent jet is in PA 50°, the line along which the components are separated.

PKS 0431 − 13·5 and 0431 − 13·3

The region of sky containing the two sources PKS 0431 − 13·5 and 0431 − 13·3 was mapped at 5000 MHz with a series of right ascension scans at intervals of 3′ arc in declination, together with a single declination scan through the peaks of the two sources. The scans, analysed on-line as described in Section II, indicate clearly that no bridge of emission joins the sources. No beam broadening is evident for PKS 0431 − 13·5, which is consistent with Fomalont's (1968) observation that the EW extent of the source is less than 0′·4 arc. Some beam broadening is evident for PKS 0431 − 13·3 along PA $20° \pm 20°$. The beam broadening is consistent with structure $\sim 2'$ arc in extent but the signal to noise ratio is poor because of the large spacings between scans. The observation is consistent with the two models proposed from interferometry (Fomalont 1968; Ekers 1969) (Table 1) and does not help to distinguish between them.

PKS 0454 − 22

The present observations of PKS 0454 − 22 show slight beam broadening indicative of structure $\sim 1'\cdot 5 \times < 1'\cdot 0$ (EW × NS).

PKS 0511 − 30

From observations of PKS 0511 − 30 with the Caltech interferometer, Fomalont (1971) proposed a three-component model. However, as in the case of PKS 0349 − 27, Fomalont's two south–western components may be a single extended emission region. Observations of the source by Ekers (1969) with the Parkes interferometer agree with the model of Fomalont and suggest that even more complex structure may be present. The 80, 408, and 5000 MHz contour maps of Lockhart (1971), Schilizzi and McAdam (1970), and the present observations (Fig. 5) respectively are from pencil beam instruments of similar resolution. They indicate a double structure, which is in basic agreement with the results from interferometry. Lockhart (1971) compared the pencil beam observations and concluded that there is little change in structure between 80 and 5000 MHz. He suggested that the north–east component has a slightly steeper spectrum than the south–west component and that the regions of low surface brightness observed to the north and south of the source at 80 MHz have steep spectra since they do not appear in either the 408 or 5000 MHz contour maps. In this respect the source may resemble PKS 0123 − 01, for which the relatively steep spectrum of the outer components was discussed by Schilizzi *et al.* (1972).

PKS 0541 − 24

The lack of beam broadening in the present observations of PKS 0541 − 24 indicates upper limits to the source dimensions of $1'\cdot 3 \times 0'\cdot 9$ (EW × NS).

PKS 0634 − 20

Pencil beam observations of the very extended source PKS 0634 − 20 were carried out by Lockhart (1971) at 80 MHz, Schilizzi and McAdam (1970) at 408 MHz, and Gardner and Whiteoak (1971) at 5000 MHz, with telescopes of similar resolving powers. From a comparison of the results, Lockhart (1971) concluded that the southern (more compact) component has a slightly steeper spectrum than the northern component. Lockhart's observations at 80 MHz indicated the presence of some outlying emission regions with relatively steep spectra. From observations with the Parkes interferometer, Ekers (1969) suggested that there may be compact components of emission along the bridge joining the two components. The present observations (Fig. 6) are in good agreement with the earlier observations from the Parkes 64 m telescope (Gardner and Whiteoak 1971) in which a 5000 MHz receiver of somewhat smaller bandwidth and larger noise figure was used. The high degree of linear polarization found by Gardner and Whiteoak (14·5% and 19·0% for the northern and southern components respectively) accounts for the differences between the peak flux densities of the components as obtained in the present work and by Shimmins *et al.* (1969). The original identification (Bolton *et al.* 1965) was classed as an elliptical galaxy but colours measured by Westerlund and Wall (1969) indicated that the object is an N galaxy. This classification is confirmed by the presence of high-excitation emission lines in the optical spectrum (Searle and Bolton 1968). The redshift of 0·056 determined by Searle and Bolton implies the large separation between components of ~500 kpc.

PKS 0800−09

Pencil beam observations of PKS 0800−09 were carried out at 80 MHz (Lockhart 1971) and 408 MHz (Schilizzi and McAdam 1970) with resolutions similar to that of the present observations. The extraordinary dependence of structure on frequency which is suggested by comparison of these observations with the present results (Fig. 7(*a*)) has been discussed by Lockhart (1971). The differences in the structures are illustrated in Figure 7(*b*), in which intensity profiles along PA 90° have been drawn from the contour maps at the three frequencies. Part of the apparent change in structure between 80 and 408 MHz may be due to the influence of the ionosphere on the 80 MHz results. The two most easterly components in the 80 MHz map are not observed at 408 MHz and, if they are real, the spectrum of these components would be steeper than any at present known. Comparison of the 408 and 5000 MHz results indicates that the component separation is larger at 5000 MHz and that the eastern component has a flatter emission spectrum than the western component. The model proposed by Ekers (1969) on the basis of 467 MHz observations with the Parkes interferometer is in good agreement with the 408 MHz observation of Schilizzi and McAdam. Moreover, the interferometer observations at 1401 MHz by Ekers provide a clear indication that the component separation increases with frequency. The identification of the source with an $18^{m}\cdot 5$ elliptical galaxy (Bolton and Ekers 1966*b*) has been questioned by Schilizzi and McAdam (1970), who point out that there are 10 cluster members within 60″ arc of the centre of the emission bridge joining the components.

PKS 0806−10

From observations of PKS 0806−10 with the Caltech interferometer at 1425 MHz, Fomalont (1971) proposed a two-component model (see Table 1) for its structure. The present observations (Fig. 8) show that the source is extended along PA 14°, which is in agreement with Fomalont's model. However, the degree of beam broadening indicates that if the two-component structure is qualitatively correct then the component separation at 5000 MHz is $\sim 2' \cdot 4$ arc, which is significantly greater than the $1' \cdot 3$ arc separation derived by Fomalont for the 1425 MHz model.

PKS 0819 – 30

From a comparison of observations of PKS 0819 – 30 at 80 MHz with observations at 408 MHz (Schilizzi and McAdam 1969) and 1425 MHz (Fomalont 1968), Lockhart (1971) concluded that there is no major change in structure over this frequency range. He suggested that in order to improve the agreement with the pencil beam observations of Schilizzi and McAdam, the three-component model suggested by Fomalont from observations with the Caltech interferometer on an EW baseline should be modified to a model of two components joined by an emission bridge. More recently a model with three Gaussian components has been proposed by Fomalont (1971) on the basis of observations on both EW and NS baselines. The presentation of the model convolved to a resolution of 45″ arc in Fomalont's Figure 6(*a*) indicates that the extended component may well represent an emission bridge between the major components. Ekers (1969) found that the results of his interferometry at 467 and 1401 MHz required a model of the emission to have either a third component or an emission bridge, which is in agreement with both Lockhart's suggestion and Fomalont's model.

The contour map of Figure 9 is very similar to that obtained at 80 MHz by Lockhart (1971) and, in particular, intensity profiles taken from the two maps along PA 126° show close agreement. Consequently there is little change in structure over the frequency range 80 to 5000 MHz. Lockhart noted that the spectrum of integrated emission for the source appears to steepen between 2650 and 5000 MHz. However, the 5000 MHz flux density which he used (from Shimmins *et al.* 1969) has been underestimated through the application of too small a correction for resolution effects. The flux density from Table 1 indicates that the integrated spectrum is well represented by a single power law between 80 and 5000 MHz.

PKS 1107 – 22

The present observations of PKS 1107 – 22 indicate that the "source" described in the Parkes catalogue as being extended or double is the two unresolved and apparently unrelated sources given in Table 1. No optical identifications could be made from an examination of the Palomar Sky Survey prints at the source positions.

PKS 1354 – 17

The present observations of PKS 1354 – 17 indicate that the "source" described in the Parkes catalogue as being extended to the south is two unresolved sources (listed in Table 1) which do not appear to be related. The position obtained for the weaker source is coincident with an $18^m \cdot 5$ blue stellar object on the prints of the Palomar Sky Survey, and the possible identification of the source with a QSO is noted in Table 1. A finding chart is given in Figure 17(*a*).

PKS 1514 – 16

The contour map of PKS 1514 – 16 shown in Figure 10 was constructed from three right ascension scans only. The small peak intensity of this source and the limited observations resulted in poor signal to noise ratio and the final map is the result of a considerable amount of smoothing. On the Palomar Sky Survey prints there is an $18^m \cdot 5$ galaxy (R.A. $15^h 14^m 51^s$, Dec. $-16° 30' \cdot 8$ (1950)) approximately $1' \cdot 5$ arc east of the emission centroid.

PKS 1518 − 29

Scans to map the region containing PKS 1518 − 29 revealed three additional sources, all of which are listed in Table 1. The four sources appear to be unrelated and are unresolved. The source of earliest right ascension (PKS 1518 − 29·5) is the catalogued source. The northernmost source (PKS 1519 − 29·4) may have a flat or inverted spectrum since it does not appear in the Parkes 408 MHz catalogue. The Palomar Sky Survey prints were examined at each of the four source positions. For PKS 1519 − 29·6, an $18^m \cdot 5$ galaxy is within the position uncertainties, and this is given as the identification in Table 1. A finding chart appears in Figure 17(*b*).

PKS 1559 + 02

From a comparison of the present observations (Fig. 11) with observations of similar resolution at 80 MHz, Lockhart (1971) concluded that the western component of PKS 1559 + 02 has a flatter spectrum than the eastern component. However, when the model of emission at 1425 MHz proposed by Fomalont (1971) is convolved to the $4' \cdot 0$ arc resolution of the present observations, there is close agreement with the brightness distribution given in Figure 11. These results imply that differences between the spectra of the components are confined to the frequency range 80 to 1425 MHz.

PKS 1949 − 01

The present observations of PKS 1949 − 01 (Fig. 12) show that the source has a double structure. Parameters of the components are given in Table 1.

PKS 2058 − 28

The two-component models of PKS 2058 − 28 derived from interferometry by Ekers (1969) and Fomalont (1971) have been convolved to the resolution of the present 5000 MHz observations (Fig. 13). The model proposed by Ekers, in which the components have an intensity ratio of 1·3, is in better agreement with the present results than the model of Fomalont, in which the component intensities are nearly equal. However, the models are consistent with each other and with the present results to within quoted errors, and little dependence of structure on frequency is suggested. Lockhart (1971) has mapped the source at 80 MHz with a pencil beam similar in width to that used in the present work. His map shows features in the structure of the southern portion of the source which are not present in the higher frequency results. Moreover, the position angle of greatest elongation is significantly different from that of Figure 13 and of the interferometry models. It is possible that the 80 MHz observation has been affected by the ionosphere, as was suggested in the case of PKS 0800 − 09.

PKS 2058 − 13

The 5000 MHz observations of PKS 2058 − 13 (Fig. 14) indicate a double structure with the components joined by a strong emission bridge. Parameters of the intensity distribution are given in Table 1.

PKS 2104 − 25

Similar two-component models for PKS 2104 − 25 were proposed from interferometry by Ekers (1969) and Fomalont (1971). However, Ekers suggested that the brightness distribution is poorly represented by a model of two Gaussian components. The present observations (Fig. 15) indicate that the southern "component" is in fact an arc-like feature, and there appear to be additional low-brightness regions to the north-west of the emission centroid. Lockhart (1971) observed the source at 80 MHz with a resolution similar to that of the present observations. The southern arc-like feature is more prominent in the 80 MHz map than in Figure 15, and a comparison of the intensity profiles along PA 135° confirms that this extended feature has a steeper spectrum than the emission nearer the intensity peak. The visibility functions obtained by Ekers (1969) also indicate a change in structure with frequency. In both PA 115° and 160° the 467 and 1401 MHz functions differ in the sense which indicates that the extended component of the brightness distribution has the steeper emission spectrum. Ekers (1969) noted that the suggested identification of PKS 2104 − 25 with a $16^m \cdot 8$ galaxy (Bolton *et al.* 1965) may be incorrect, since there are brighter ($\sim 14^m$) galaxies within the brightness contours. There are no prominent emission lines in the optical spectra of these galaxies, or in the spectrum of the $16^m \cdot 8$ galaxy suggested as the identification (J. G. Bolton, personal communication).

PKS 2149 − 20

The lack of beam broadening in the present observations of PKS 2149 − 20 indicates upper limits to the source dimensions of $0' \cdot 6 \times 0' \cdot 6$ (EW × NS).

PKS 2221 − 02

A model of PKS 2221 − 02 consistent with the double structure interpretations from interferometry given by Maltby and Moffet (1962) and Fomalont (1968) consists of two Gaussian components separated by $\sim 4'$ arc along PA $\sim 165°$. However, the present observations (Fig. 16) indicate that the overall extent of the brightness distribution must be at least $6'$ arc along PA 173°. Moreover, components were not resolved along this position angle and, if a two component model is valid, the components must be extended or linked by a strong emission bridge. Alternatively several regions of emission are present. The source was observed at 80 MHz by Lockhart (1971), who was also unable to resolve it into individual components. The northern half of Lockhart's contour map closely resembles that of Figure 16. However, as in the case of PKS 2058 − 28, the southern halves show considerable dissimilarity and it is suggested that in this region the 80 MHz brightness distribution given by Lockhart reflects some ionospheric effects.

PKS 2329 − 16

The present observations indicate that the "source" listed in the Parkes catalogue as PKS 2329 − 16 is actually the two unrelated and unresolved sources given in Table 1. The emission spectrum of the stronger source is very flat in the frequency range 1410 to 5000 MHz. The Palomar Sky Survey prints were examined at the two source positions. An $18^m \cdot 5$ N galaxy is close to the position measured for the stronger source, and is given as the identification in Table 1. A finding chart is shown in Figure 17(*c*).

V. Acknowledgments

We are grateful to Mr. A. J. Shimmins for help in calibration of the telescope pointing, and for the development of the sampling and filtering subroutines used in the computer program for the on-line analysis of the data. We thank Mr. J. G. Bolton for valuable discussions.

VI. References

Bolton, J. G., Clarke, Margaret E., and Ekers, R. D. (1965).—*Aust. J. Phys.* **18**, 627.
Bolton, J. G., and Ekers, Jennifer (1966*a*).—*Aust. J. Phys.* **19**, 559.
Bolton, J. G., and Ekers, Jennifer (1966*b*).—*Aust. J. Phys.* **19**, 713.
Cameron, M. J. (1971).—*Mon. Not. R. astr. Soc.* **152**, 439.
Ekers, R. D. (1969).—*Aust. J. Phys. astrophys. Suppl.* No. 6.
Fomalont, E. B. (1968).—*Astrophys. J. Suppl. Ser.* **138**, 203.
Fomalont, E. B. (1971).—*Astr. J.* **76**, 513.
Gardner, F. F., and Whiteoak, J. B. (1971).—*Aust. J. Phys.* **24**, 899.
Lockhart, I. A. (1971).—Ph.D. Thesis, Australian National University.
McVittie, G. C. (1965).—*Astrophys. J.* **142**, 1637.
Maltby, P., and Moffet, A. T. (1962).—*Astrophys. J. Suppl. Ser.* **7**, 141.
Mills, B. Y. (1955).—*Aust. J. Phys.* **8**, 368.
Mills, B. Y. (1960).—*Aust. J. Phys.* **13**, 550.
Schilizzi, R. T., and McAdam, W. B. (1969).—*Proc. astr. Soc. Aust.* **1**, 228.
Schilizzi, R. T., and McAdam, W. B. (1970).—*Proc. astr. Soc. Aust.* **1**, 337.
Schilizzi, R. T., Lockhart, I. A., and Wall, J. V. (1972).—*Aust. J. Phys.* **25**, 545.
Searle, L., and Bolton, J. G. (1968).—*Astrophys. J.* **154**, L101.
Shimmins, A. J. (1968).—*Aust. J. Phys.* **21**, 65.
Shimmins, A. J., and Bolton, J. G. (1972).—*Aust. J. Phys. astrophys. Suppl.* No. 23.
Shimmins, A. J., Clarke, Margaret E., and Ekers, R. D. (1966).—*Aust. J. Phys.* **19**, 649.
Shimmins, A. J., Manchester, R. N., and Harris, Beverley J. (1969).—*Aust. J. Phys. astrophys. Suppl.* No. 8.
Slee, O. B. (1972).—*Astrophys. Lett.* **12**, 75.
Wall, J. V., Cole, D. J., and Milne, D. K. (1968).—*Proc. astr. Soc. Aust.* **1**, 98.
Westerlund, B. E., and Wall, J. V. (1969).—*Astr. J.* **74**, 335.